Electron confinement in hexagonal vacancy islands: Theory and experiment

L. Niebergall, G. Rodary, H. F. Ding,* D. Sander, V. S. Stepanyuk, P. Bruno, and J. Kirschner
Max-Planck-Institut für Mikrostrukturphysik, Weinberg 2, D-06120 Halle/Saale, Germany
(Received 20 July 2006; revised manuscript received 18 September 2006; published 28 November 2006)

Electron confinement in hexagonal vacancy islands on Cu(111) is studied by state of the art *ab initio* calculations and experimentally by low-temperature scanning tunneling spectroscopy measurements (STS). Both theory and experiment reveal standing wave patterns of the local density of states (LDOS), which are ascribed to the scattering of surface-state electrons at the boundary of the vacancy island. The spatial modulation of the LDOS, its size, and energy dependence as measured by STS are well reproduced by our calculations. This agreement between theory and experiment corroborates the application of our theoretical approach to other confined systems, including spin-polarized effects. Our studies predict that quantum states of vacancy islands with magnetic adatoms can be used to tailor the spin-polarization of surface-state electrons on metal surfaces.

DOI: 10.1103/PhysRevB.74.195436 PACS number(s): 73.20.At, 72.10.Fk

I. INTRODUCTION

Electron confinement at nanoscale structures has been investigated both theoretically[1–3] and experimentally by scanning tunneling microscopy (STM) and spectroscopy (STS). Examples are electron confinement at step edges of terraces,[4–7] within quantum corrals,[8–12] in islands,[13–17] in monoatomic chains,[18,19] and in vacancy islands.[20] In these examples, surface-state electrons are scattered at the boundary of the confining structure, and standing-wave patterns of the electron local density of states (LDOS) have been observed as spatial modulation of the differential conductance (dI/dU, I: tunneling current, U: gap voltage U_{gap}) by STS.

These spatial modulation of the LDOS are of great interest for atomic manipulation on the nanoscale. Tailoring LDOS modulation opens new ways to steer and manipulate atomic diffusion,[21] and it has been shown to determine interactions between ad-atoms.[22] Recent theoretical work has identified that electron confinement depends on the electron spin-polarization, and the resulting LDOS standing wave pattern of ferromagnetic systems are calculated to be spin-polarized.[23]

In view of the potential applications of using LDOS modulation patterns for atomic and spin manipulation, elaborate theoretical models have to be developed and tested to describe the underlying electron scattering processes. In peculiar, predictions of the resulting LDOS pattern and its spin-polarization are called for. This presents a formidable task as only for few selected systems, such as terraces and circular and triangular shapes, analytical solution of the corresponding boundary value problems are known for the simplification of an infinite hard wall quantum box.

The theoretical description for slightly more complicated systems, however, requires a much more demanding effort. A variational embedding technique has been developed to calculate the LDOS of hexagonal systems on Ag(111);[20,24,25] albeit it requires that the level broadening of the LDOS spectra is included on an empirical basis.

Here we present conclusive evidence in support of our recently developed model[23,26] to calculate electron confinement in an hexagonal system. Not only does the calculation reproduce the spatial modulation pattern of the resulting LDOS standing waves within hexagonal vacancy islands, it also reproduces the energy dependence of the LDOS as measured by low-temperature (LT-) STM and LT-STS. Our theoretical approach represents an advance in the description of electron confinement, as it does not require an *a priori* assumption of the energetic width of the peaks of the calculated LDOS, but it reproduces the overall LDOS spectra without further assumptions satisfactorily.

It is the goal of this study to use our STS data on electron confinement in hexagonal vacancy islands on Cu(111) as a benchmark for our theoretical approach[26] to describe confinement effects with an *ab initio*-based method. Our results reveal that the electron scattering at a monolayer high step at the inner edge of the Cu vacancy island can be modeled as the scattering due to a Cu corral (see Fig. 1) of the same size as the vacancy island. The good agreement between theory and experiment regarding the spatial modulation pattern of the LDOS, its amplitude, and its spectroscopic features corroborates the applicability of our model to study also spin-polarized electron confinement. As an outlook, we also address the spin-dependence of the electron confinement.[27]

II. PREVIOUS WORK: EIGENSTATES AND FINITE WIDTH OF ENERGY LEVELS

Electron confinement in vacancy islands has been studied in the past both by experiment and theory. In this section, we discuss the aspects in which our combined experimental and theoretical work advances the physical description of electron confinement with respect to previous work. Our approach does not rely on specific assumptions and empirical input data, which were part of previous theoretical work. One main advance of our DFT calculation with respect to previous work[20,25] is that starting from *one* model we can tackle relevant aspects of electron confinement, such as spatial modulation of the LDOS, energy levels of a confined system, and finite energy width of the energy levels in *one* coherent description.

We focus on three aspects that describe electron confinement in nanostructures, namely, the spatial modulation of the

LDOS, the energy position of eigenstates, and the energy width of the peaks of the dI/dU spectra.

Previous work has indicated that peaks of dI/dU spectra can be ascribed to eigenstates of electrons in a confined system. Certain simplifications have been employed previously to calculate the eigenenergies of a hexagonal confined system. A variational embedding scheme[24] has been used to calculate the energy of eigenstates of a particle in a hexagonal box, where the confinement to the hexagonal domain was ascribed to *infinitely* high potential barriers.[25] This approach has the benefit of giving the eigenvalues as $E_n = E_0 - \lambda_n/(m^*\Omega)$, where E_0 is energy offset of the surface state from the Fermi level, and the electron effective mass is m^*, and the hexagon area is given by Ω. The values of λ_n are tabulated in Ref. 25.

Certain simplifications have been employed previously to describe the lifetime of surface state electrons confined to different nanostructures on Ag(111).[20] In this previous study, experimental dI/dU spectra have been fitted by a series of Lorentzian curves to extract the peak width (lifetime), as a function of electron energy. The data led the authors to the conclusion that the geometric shape of the confined system had little impact on the lifetime, and they considered a circular vacancy island to discuss lifetime effects in hexagonal and triangular systems. A phenomenological model has been employed to derive an analytical expression for the width of an energy level. The authors model the electron lifetime by considering two contributions, which are due to lossy scattering at the boundary of the circular vacancy island (reflection coefficient at border of confinement <1) and in-elastic scattering (electron-electron and electron-phonon scattering).[20] The authors conclude that lossy scattering is, by far, the most dominant decay channel as compared to in-elastic electron scattering.

Our DFT calculations take scattering of Cu surface state electrons into Cu bulk states into account. This loss of surface state electrons into bulk states is equivalent with a limited lifetime of surface state electrons, thus it induces a peak broadening of the LDOS. The following discussion of our results indicates that our calculations give a favorable agreement between experimental STS and calculated LDOS data. Important aspects of electron confinement, such as spatial modulation of the LDOS, energy position of peaks of LDOS as a function of energy, and their width, are all calculated in close agreement with experimental results. From this we conclude that electron scattering into bulk states is a key factor, which determines LDOS peak widths in our system.

In conclusion, the comparison of our present DFT calculation with previous theoretical work based on the variational embedding scheme and on circular shape structures indicates, that both approaches lead to a proper description of the experimental results. However, our present calculational scheme arrives at a proper description of the spatial modulation of the LDOS, the energy levels, and the finite line width of the energy levels starting from *one* model. This contrasts with previous work, where different aspects of electron confinement (spatial modulation of the LDOS, energy levels, finite width of energy levels) have been tackled separately with specialized models, which relied on various simplifications and empirical input.

III. EXPERIMENTAL

Vacancy islands on Cu(111) are an ideal playground to study electron confinement as they form with a wide range of sizes on submonolayer deposition of Fe,[28] Co,[29] or Ni.[15] The metal deposition leads to the outdiffusion of Cu surface atoms, which leaves monolayer deep depressions with often nearly perfect hexagonal shapes behind. Electron confinement of Cu surface-state electrons results from the electron scattering at the boundary of the vacancy island. We prepare vacancy islands on Cu(111) by depositing submonolayer quantities of Co at room temperature. The Co-induced vacancy islands have a distribution of sizes from a few nanometers up to 25 nm, and they often exhibit an almost regular hexagonal shape, as depicted in Figs. 1–3. We define the vacancy islands size d as the distance between two opposite edges, measured at a half step height, as indicated in Fig. 1.

Before Co deposition, the Cu(111) crystal is prepared by cycles of ion bombardment (Ar^+, 1 keV, 1 μA) and subsequent annealing at 700 K (15 min), which produces atomically flat terraces, separated by mainly monoatomic steps, as checked *in situ* by STM. Note that the clean Cu(111) surface does not show hexagonal vacancy islands. STS on the clean Cu(111) surface identifies the onset of the surface state band at 0.44 ± 0.01 eV below the Fermi energy with an effective electron mass $m^* = 0.39 \pm 0.01 m_e$ (m_e: electron mass), in agreement with previous work.[4]

Measurements of the morphology and the electronic properties of vacancy islands are performed with an ultrahigh vacuum (UHV) STM at a temperature of 7 K. The STM tip is cut from an Ir wire, and it is treated *in situ* by voltage pulses of several volts and soft indentation into the Cu surface to sharpen its apex. For topogrophic imaging, the STM is operated at a fixed current of 1 nA and gap voltages U_{gap} between -1 and $+1$ V, where a positive voltage corresponds to electron tunneling from the tip into the sample. Scanning tunneling spectroscopy (STS) is performed to study the electron local density of states with high spatial resolution above the vacancy island. STS measurements are performed by modulating the gap voltage U_{gap} with an ac voltage of 5 mV amplitude at a frequency of 4 kHz, and detecting the resulting ac signal of the tunnel current with a lock-in amplifier. This spectroscopic signal corresponds to the differential conductance dI/dU, and it reflects the LDOS at the energy eU_{gap}.[2]

IV. THEORY

Our *ab initio* calculations are based on the density functional theory (DFT) in the local spin-density approximation and multiple-scattering approach using the Korringa-Kohn-Rostocker (KKR) Green's function (GF) method.[23,26]

The basic idea of the method is a hierarchical scheme for the construction of the Green's function of quantum resonators (vacancy islands, nanoislands, corrals) on a metal surface by means of successive applications of Dyson's equation. We treat the surface as the two-dimensional perturbation of the bulk. Taking into account the 2D periodicity of the ideal surface, we find the structural Green's

function by solving a Dyson equation self-consistently

$$G^{jj'}_{LL'}(\mathbf{k}_\parallel,E) = \mathring{G}^{jj'}_{LL'}(\mathbf{k}_\parallel,E) + \sum_{j''L''} \mathring{G}^{jj''}_{LL''}(\mathbf{k}_\parallel,E)\Delta t^{j''}_{L''}(E)G^{j''j'}_{L''L'}(\mathbf{k}_\parallel,E). \quad (1)$$

Here $\mathring{G}$ is the structural Green's function of the bulk in a $\mathbf{k}_\parallel$-layer representation (j,j'-layer indices). The $\mathbf{k}_\parallel$ wave vector belongs to the two-dimensional (2D) Brillouin zone. $\Delta t^j_L(E)$ is the perturbation of the t matrix to angular momentum $L=(l,m)$ in the jth layer.

The structural Green's function of the ideal surface in a real-space representation is then used as the reference Green's function for the calculation of the Green's function of a quantum resonator by means of a Dyson equation

$$G^{nn'}_{LL'}(E) = \mathring{G}^{nn'}_{LL'}(E) + \sum_{n''L''} \mathring{G}^{nn''}_{LL''}(E)\Delta t^{n''}_{L''}(E)G^{n''n'}_{L''L'}(E),$$

where $G^{nn'}_{LL'}(E)$ is the energy-dependent structural Green's function matrix and $\mathring{G}^{nn''}_{LL''}(E)$ the corresponding matrix for the ideal surface, serving as a reference system. $\Delta t^n_L(E)$ describes the difference in the scattering properties at site n induced by the existence of the resonator. Exchange and correlation effects are included in the local density approximation. The full charge density is used in our calculations. Our studies have proved that in the present case, i.e., for vacancy islands on Cu(111), only a limited number of atoms near the side wall of the vacancy island contribute to $\Delta t^n_L(E)$ and to the interference patterns inside the vacancy island. Therefore, the vacancy island can be well approximated by the hexagonal corral, as shown schematically in Fig. 1. Phase shifts on scattering are calculated fully self-consistently. Our calculations take scattering of the surface state electrons into bulk states into account.

Our calculations rely on a model structure, which is sketched in Fig. 1(c). The 7 nm vacancy island of Fig. 1(a) is modeled in the calculation by an hexagonal Cu corral composed of Cu ad-atoms in threefold coordinated sites, with 17 atoms along one side, which results in a size of $d=7.08$ nm. The following discussion of our experimental and theoretical results supports the important result of this work that electron scattering within a Cu depression of a given size can be treated as electron confinement in a Cu corral of the same size.

We have also checked the effect of the second shell of adatoms forming a double-walled corral on our results. We have found that the peak positions in the LDOS and their half widths are practically identical for a single-walled and a double walled corral. This result is in agreement with a experimental study where electron confinement in single-walled and double-walled ring of Fe atoms on Cu(111) has been studied.[10] The experimental spectra reveal the same half width and only a minute energy shift by 5–10 meV for confinement in a single-as compared to a double-walled system.

V. RESULTS: COMPARISON BETWEEN EXPERIMENT AND THEORY

In the following, we present two important aspects of the electron confinement in nanostructures, namely, the energy dependence of the spatial variation of the LDOS within a hexagonal vacancy island (Fig. 2) and the LDOS as a function of energy for different vacancy island sizes (Fig. 3).

Figure 1(a) shows a STM topography image of an hexagonal vacancy island. The line scans of Fig. 1(b) indicate a vacancy island size at half depth of 7 nm for one line scan. The line scans also reveal a slight modulation of the apparent height at the bottom of the vacancy island, which is due to the formation of electron standing waves within the vacancy island. These apparent height modulations are ascribed to local variations of the LDOS, which are more pronounced in the spectroscopy images of the differential conductance in Fig. 2.

Figure 2 presents, in the left column, experimental data of the differential conductance dI/dU by STS. Brighter colors reflect a larger value of dI/dU. The black hexagons mark the vacancy island position as obtained by STM. The label gives the gap voltage, which is varied between −0.3 V (top), −0.2 V (center), and +0.1 V (bottom). The images show that with increasing voltage the spatial modulation of dI/dU map reveals more structure. At low negative voltage, a ringlike intensity variation is measured, whereas with increasing voltage, an azimuthal contrast evolves, which shows a clear sixfold symmetry at +0.1 V. Also, the brightness at the center position changes from a minimum to a maximum. The center column of Fig. 2 shows the calculated LDOS (calculated at a height of 0.5 nm above the Cu surface) at energies E_F −0.3 eV (top), E_F−0.2 eV (center), and E_F+0.1 eV (bottom). A brighter color indicates a larger value of the LDOS. Clearly, the visual comparison between experimental and calculated values identifies a close agreement between them. To illustrate the comparison, we show, in the right column, a horizontal line scan through the center positions of the maps, as indicated by the line in the top images. The experimental data are given by individual symbols, and the calculated values are given by the solid line. Each plot has been shifted vertically to have the same value at the center position and scaled vertically to have the same value at the first maximum (top panel) or minimum (lower two panels). The comparison between experiment and theory reveals that the calculation reproduces the position of the minima and maxima properly with only small deviations of the order of 0.1 nm. Also, the variation of the relative intensity with position is reproduced qualitatively.

The spatial variation of the differential conductance depends also on the size of the vacancy island. Figure 3 shows measurements of the differential conductance dI/dU by STS for hexagonal vacancy islands with sizes between 4.3 nm (top) and 10.6 nm (bottom), where the solid hexagons mark the vacancy island position and size. The left column gives the STS image at the indicated gap voltage. The voltage is chosen at the value given by a maxima in the spectrum measured at the center position of the vacancy islands for varying U_{gap} from −0.6 to +0.6 V. The dI/dU spectra of the center column show that more maxima evolve with increasing

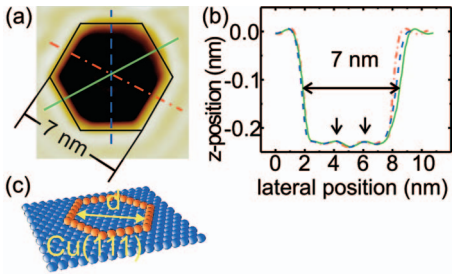

FIG. 1. (Color) (a) Topographic STM image of a 7 nm size vacancy island on Cu(111) (U_{gap}=−0.02 V, I=0.5 nA). The line scans of (b) are given by the lines. (b) The line scans reveal the monolayer deep depression (0.21 nm) and two apparent modulations (arrows) due to the impact of the electron standing waves on the topographic image. The depression has a size of 7 nm, which varies by ~0.1–0.2 nm, along different scan directions. (c) A corral of Cu adatoms on Cu(111) with the same size d as the depression is used in the calculations to model the vacancy island of (a).

U_{gap}. The position of the maxima move to smaller energy with decreasing size. A common detail of all spectra is the decay of the intensity at negative U_{gap} below −0.4 V. This decay is due to the onset of the surface state band of Cu(111), which is located 0.44 V below the Fermi energy. A band gap is observed for more negative values, and no occupied surface states of Cu are available for tunneling into the tip, which causes a drop of the differential conductance.

Also, the dI/dU curves reside on a background that decays with increasing voltage. This overall background signal is similar to the surface-state spectrum obtained on clean Cu(111). The decay of the background signal with increasing voltage is due to the energy dependence of the LDOS of the tip.[30] In the calculation shown in the right column, only the LDOS of the sample is considered and the tip effect is neglected.

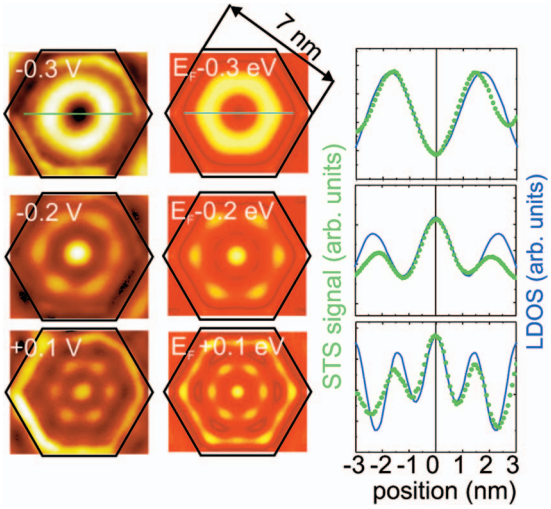

FIG. 2. (Color) STS images of dI/dU at the indicated gap voltage at 1 nA (left column) and the calculated LDOS at various energies of the 7 nm vacancy island of Fig. 1. The solid hexagon marks the vacancy island rim as in Fig. 1. The right column shows horizontal line scans along the center of the vacancy island, as indicated by the green line for different energies. Solid line: calculation (center column), symbols: experimental data (left column).

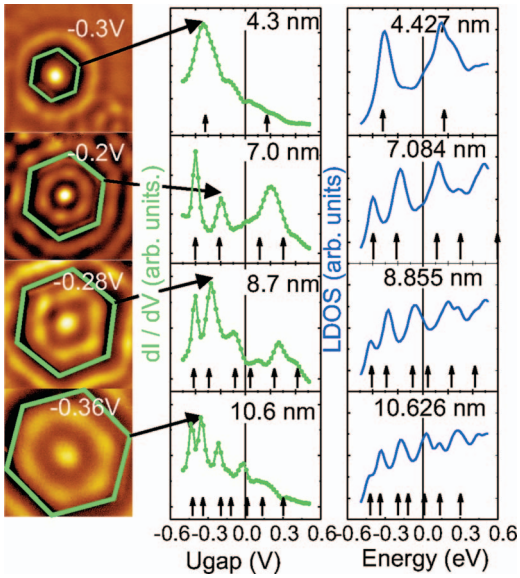

FIG. 3. (Color) Left column: STS images of vacancy islands of different size of 4.3–10.6 nm as indicated on the center column plots, at various U_{gap}, as given on the left column (I=1 nA). Center column: Spectroscopy dI/dU at center position of the vacancy islands (stabilization parameters: U_{gap}=−1 V, 1 nA). Right column: calculated LDOS spectra. The arrows indicate the energy levels E_n as adopted from an analytical model (Ref. 20). With increasing vacancy island size, more energy levels appear that correspond to the levels n=1,4,10,13,20,26,32, with increasing energy.

The calculated LDOS spectra for structures of the indicated size are shown in the right column of Fig. 3. The calculations reproduce the experimentally found increase of number of maxima in the LDOS for larger islands. The number of peaks and their positions are reproduced by our calculation.

The maxima in the spectra can be tentatively identified with eigenstates of a hexagonal confined system of the indicated sizes. In calculating the energy levels, we follow the approach in Refs. 20 and 25 and calculate the eigenenergies

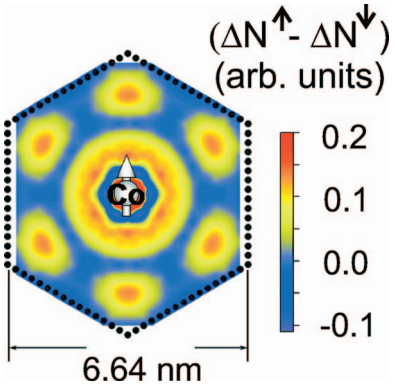

FIG. 4. (Color) Magnetic mirages in the vacancy island. A magnetic Co adatom is placed at the center of the vacancy island with R=6.64 nm. $N\uparrow$ and $N\downarrow$ are the LDOS for majority and minority electrons. $\Delta N\downarrow$ and $\Delta N\uparrow$ are determined by the difference between LDOS at the energy E_F between the vacancy island with the Co adatom and the empty vacancy island.

due to electron confinement in hexagonal vacancy islands on Cu(111) ($E_0=-440$ meV, $m^*=0.38m_e$) and the resulting energy values are given by the arrows of Fig. 3. The favorable agreement between peak positions of our calculated LDOS and those indicated by the arrows in comparison to our experimental data indicates that both calculational schemes, the variational embedding method and our DFT-based approach, give a proper description of the eigenenergies.

The arrows give the calculated position of the energy levels, which correspond to those eigenstates with a nonzero amplitude at the center of the vacancy island. The authors proposed[20] that these eigenstates are expected to be mainly responsible for the measured STS above the center of a confining structure.

The experimentally observed peak width of the LDOS on Cu(111) is well reproduced by our DFT calculation, as shown in Fig. 3. This favorable description of the LDOS of the confined system has been obtained without any empirical fitting parameter, whereas an empirically determined self-energy needs to be invoked in the variational embedding scheme to address peak broadening, as has been discussed for Ag(111).[20,25] Our DFT calculations do not rely on empirical input to produce proper line shapes.

VI. CONCLUSION AND OUTLOOK

The previous study[20,25] on Ag(111) suggested that lossy scattering is, by far, the most important decay channel that induces the measured peak width of the STS data. Our DFT calculation on Cu(111) suggests that scattering into bulk states is decisive, and so the question arises as to what extent the observed line widths of the LDOS can be ascribed to a certain decay channel. Our calculations have not been focused on a detailed lifetime study, but rather on spin-dependent confinement effects, and we cannot present an in-depth discussion of this issue here. Our DFT calculations take scattering into bulk states into account; we do not consider electron-electron and electron-phonon interactions. We are inclined to conclude from our favorable agreement between theory and experiment that these in-elastic decay channels are not the major factors that induce the finite linewidth of the energy levels of confined surface state electrons on Cu(111) at 7 K.

Finally, our studies provide a demonstration that quantum states of vacancy islands can be exploited to project the spin-polarization of a 2D electron gas to a remote location. To demonstrate this effect, we place in our calculations a magnetic Co adatom at the center of the hexagonal vacancy island and calculate the spin-polarization of the 2D electron gas inside the vacancy island. Results presented in Fig. 4 reveal that the spin-polarization of the 2D electron gas is enhanced far away from the Co adatom. The existence of "magnetic mirages" of the Co adatom is revealed. The resonance scattering of surface-state electrons from the Co adatom and from the wall of the vacancy island is found to cause this effect, which is similar to a single mirage found at the empty focus of the elliptical corral.[11,26]

In conclusion, we have presented combined theoretical and experimental studies of quantum confinement of surface-state electrons in vacancy islands on Cu(111). Our state-of-the-art *ab initio* approach has allowed us to calculate quantum states of large vacancy islands in good agreement with the experiment. Our findings indicate that the ability to exploit quantum states of vacancy islands on substrates with surface states can open exciting possibilities for the investigation of individual spins, their interactions, and the Kondo effect. Magnetic mirages of the magnetic adatom placed in the vacancy island are resolved by *ab initio* calculations.

*Present address: Department of Physics, Nanjing University, Nanjing, China (210093).

[1] H. K. Harbury and W. Porod, Phys. Rev. B **53**, 15455 (1996).
[2] G. A. Fiete and E. J. Heller, Rev. Mod. Phys. **75**, 933 (2003).
[3] S. Crampin, H. Jensen, J. Kröger, L. Limot, and R. Berndt, Phys. Rev. B **72**, 035443 (2005).
[4] M. F. Crommie, C. P. Lutz, and D. M. Eigler, Nature (London) **363**, 524 (1993).
[5] Y. Hasegawa and P. Avouris, Phys. Rev. Lett. **71**, 1071 (1993).
[6] J. Li, W.-D. Schneider, and R. Berndt, Phys. Rev. B **56**, 7656 (1997).
[7] L. Bürgi, O. Jeandupeux, A. Hirstein, H. Brune, and K. Kern, Phys. Rev. Lett. **81**, 5370 (1998).
[8] M. F. Crommie, C. P. Lutz, and D. M. Eigler, Science **262**, 218 (1993).
[9] E. J. Heller, M. F. Crommie, C. P. Lutz, and D. M. Eigler, Nature (London) **369**, 464 (1994).
[10] M. F. Crommie, C. P. Lutz, D. M. Eigler, and E. J. Heller, Surf. Rev. Lett. **2**, 127 (1995).
[11] H. C. Manoharan, C. P. Lutz, and D. M. Eigler, Nature (London) **403**, 512 (2000).
[12] K.-F. Braun and K.-H. Rieder, Phys. Rev. Lett. **88**, 096801 (2002).
[13] P. Avouris, I. Lyo, R. Walkup, and Y. Hasegawa, J. Vac. Sci. Technol. B **12**, 1447 (1993).
[14] J. Li, W.-D. Schneider, R. Berndt, and S. Crampin, Phys. Rev. Lett. **80**, 3332 (1998).
[15] S. Pons, P. Mallet, and J.-Y. Veuillen, Phys. Rev. B **64**, 193408 (2001).
[16] L. Diekhöner, M. A. Schneider, A. N. Baranov, V. S. Stepanyuk, P. Bruno, and K. Kern, Phys. Rev. Lett. **90**, 236801 (2003).
[17] S. Pons, P. Mallet, L. Magaud, and J. Veullien, Europhys. Lett. **61**, 375 (2003).
[18] S. Fölsch, P. Hyldgaard, R. Koch, and K. Ploog, Phys. Rev. Lett. **92**, 056803 (2004).
[19] F. E. Olsson, M. Persson, A. G. Borisov, J.-P. Gauyacq, J. Lagoute, and S. Fölsch, Phys. Rev. Lett. **93**, 206803 (2004).
[20] H. Jensen, J. Kroger, R. Berndt, and S. Crampin, Phys. Rev. B **71**, 155417 (2005).
[21] V. S. Stepanyuk, N. Negulyaev, L. Niebergall, R. Longo, and P. Bruno, Phys. Rev. Lett. **97**, 186403 (2006).
[22] L. Bürgi, N. Knorr, H. Brune, M. Schneider, and K. Kern, Appl.

Phys. A: Mater. Sci. Process. **75**, 141 (2002).
[23] L. Niebergall, V. S. Stepanyuk, J. Berakdar, and P. Bruno, Phys. Rev. Lett. **96**, 127204 (2006).
[24] S. Crampin, M. Nekovee, and J. E. Inglesfield, Phys. Rev. B **51**, 7318 (1995).
[25] J. Li, W.-D. Schneider, S. Crampin, and R. Berndt, Surf. Sci. **422**, 95 (1993).
[26] V. S. Stepanyuk, L. Niebergall, W. Hergert, and P. Bruno, Phys. Rev. Lett. **94**, 187201 (2005).
[27] L. Magaud, A. Pasturel, P. Mallet, S. Pons, and J.-Y. Veuillen, Europhys. Lett. **67**, 90 (2004).
[28] M. Klaua, H. Höche, H. Jenniches, J. Barthel, and J. Kirschner, Surf. Sci. **381**, 106 (1997).
[29] J. de la Figuera, J. E. Prieto, C. Ocal, and R. Miranda, Phys. Rev. B **47**, 13043 (1993).
[30] G. Hörmandinger, Phys. Rev. B **49**, 13897 (1994).